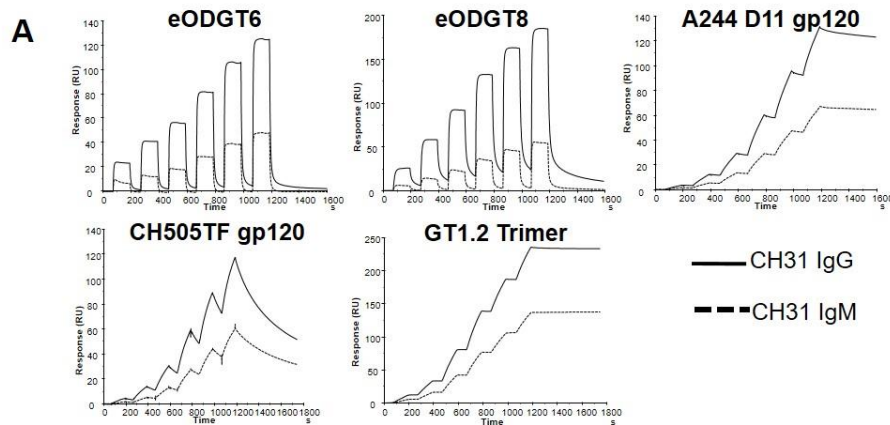


**Supplemental information**

**B cells expressing IgM B cell receptors of HIV-1  
neutralizing antibodies discriminate antigen  
affinities by sensing binding association rates**

**Md. Alamgir Hossain, Kara Anasti, Brian Watts, Kenneth Cronin, Ronald Derking, Bettina Groschel, Advaiti Pai Kane, R.J. Edwards, David Easterhoff, Jinsong Zhang, Wes Rountree, Yaneth Ortiz, Kevin Saunders, William R. Schief, Rogier W. Sanders, Laurent Verkoczy, Michael Reth, and S. Munir Alam**

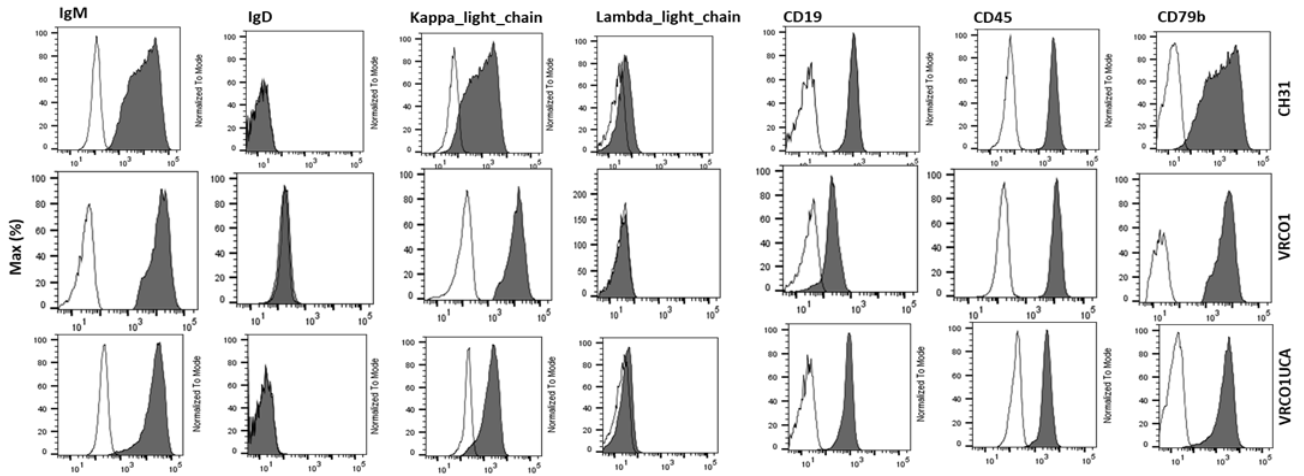
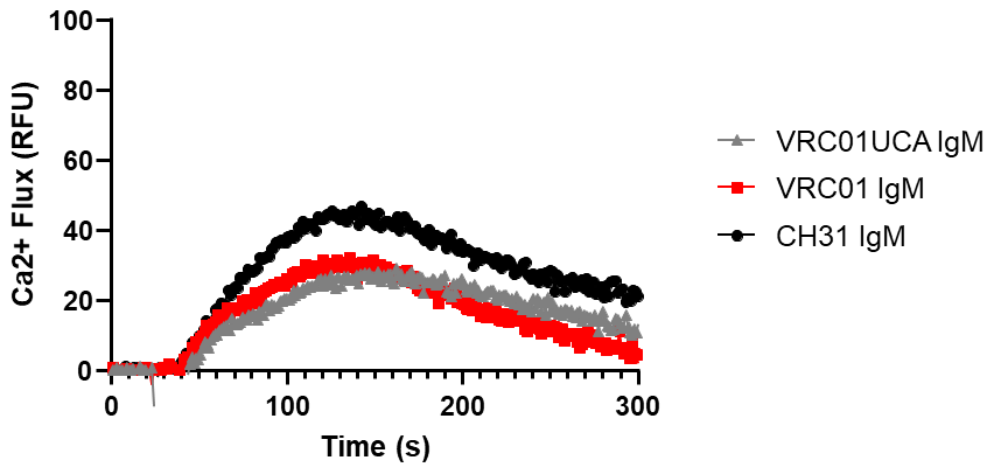
## Supplemental Information



**B**

Ag	Ab	$k_a$ (1/Ms)	$k_d$ (1/s)	$K_D$ (nM)
GT6	CH31 IgG	2.1E+4	1.2E-1	5,500
	CH31 IgM	2.2E+4	2.5E-1	11,000
GT8	CH31 IgG	1.3E+5	1.2E-1	932
	CH31 IgM	2.0E+5	2.4E-1	1,222
A244	CH31 IgG	1.4E+3	1.1E-4	78.7
	CH31 IgM	1.0E+3	7.0E-5	67.7
CH505TF	CH31 IgG	4.1E+3	7.1E-3	1,713
	CH31 IgM	1.5E+3	7.1E-3	4,743
GT1.2 Trimer	CH31 IgG	6.8E+4	<1.0E-5	<1.0
	CH31 IgM	5.5E+4	<1.0E-5	<1.0

**Figure S1. Affinity and kinetic rates of Env proteins binding to CH31 IgM mAb compared to CH31 IgG, Related to Figure 1 and STAR Methods.** (A) SPR single cycle kinetic binding profiles of monomeric (or trimeric) antigens against CH31 IgG and CH31 IgM. Plots are representative of two measurements. (B) Summary of the overall binding affinities ( $K_D$ , nM) as well as the individual kinetic rate measurements ( $k_a$  and  $k_d$ ) of each antigen with either CH31 IgG or CH31 IgM. Values are representative of two data sets. A comparison of the binding results of the monomeric antigens (GT6, GT8, A244, and CH505TF) as well as the trimeric antigen, GT1.2, suggested that the affinities and kinetic rate parameters were similar for both isoforms of CH31.

**A****B****Anti-human IgM Fab2**

**Figure S2. Ramos cell line phenotypic data and activation with control stimulant, Related to Figure 2 and STAR Methods.** (A) Representative flow cytometry plots showing expression of surface markers in bnAbs IgM (CH31, VRC01 and VRC01UCA) expressing Ramos cells (dark) with unstained control (clear). Around  $1.0 \times 10^6$  cells were fixed and stained for the surface expression of IgM, IgD,  $\kappa$ -light chain,  $\lambda$ -light chain, CD19, CD45, CD79b using fluor conjugated antibody and analyzed by BD LSR II flow cytometer. (B) Calcium flux of the following 3 Ramos cell lines: VRC01UCA IgM (gray), VRC01 IgM (red), and CH31 IgM (black) by the positive control stimulant Anti-human IgM F(ab')<sub>2</sub> at 50  $\mu$ g/mL. The fluorescence of a blank well containing only RPMI/dye was used for background subtraction. The calcium flux profiles are representative of at least two measurements and demonstrate the functionality of the three cell lines.

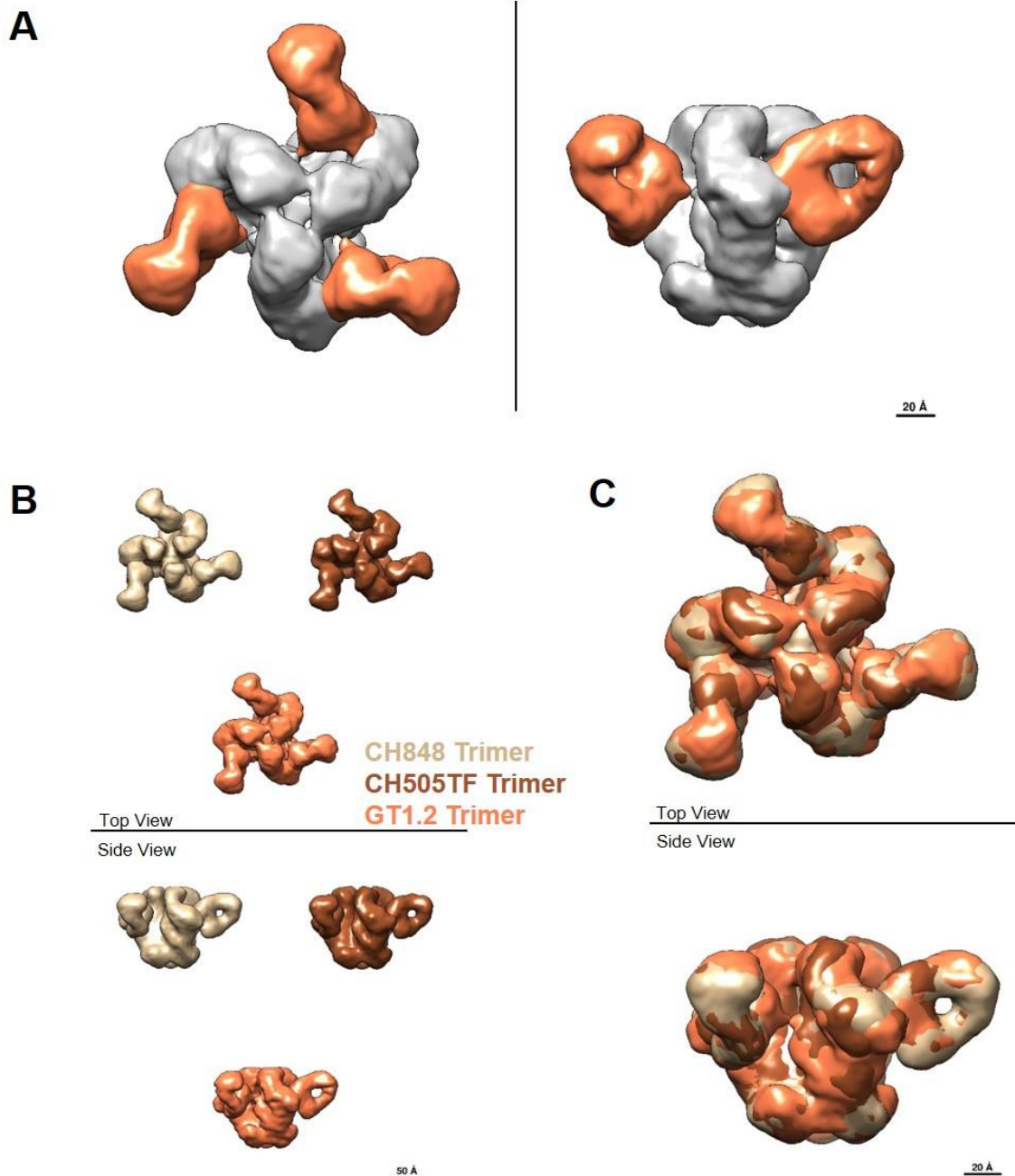
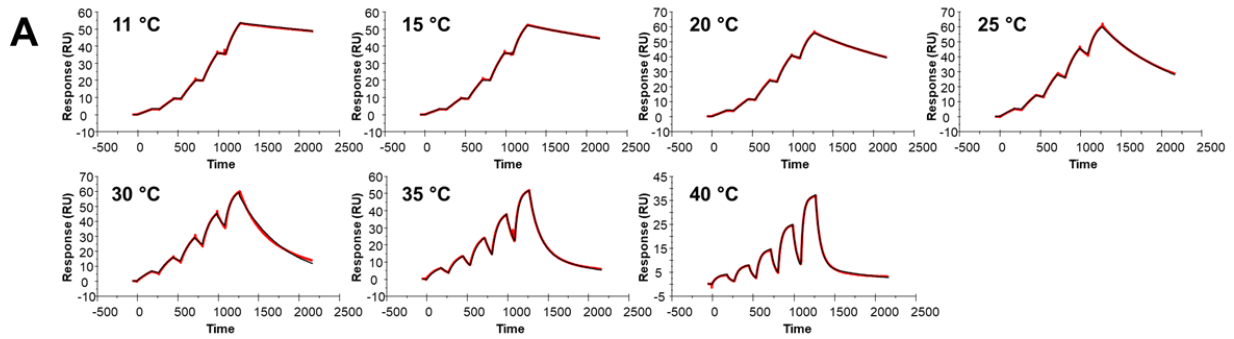
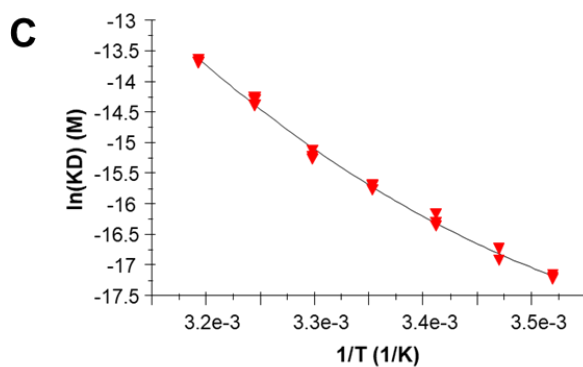


**Figure S3. Negative stain-EM structures of CH31 Fab complexed to three different SOSIP trimers, Related to Figure 1 and STAR Methods.** (A) Structure of CH31 Fab bound to GT1.2 trimer, shown in top view and side view, with the density corresponding to the Env trimer colored gray and the density corresponding to the three Fabs colored orange. (B) Side by side comparison of the structures of CH31 Fab bound to CH848, CH505TF and GT1.2 trimers, colored tan, brown and orange, respectively. (C) Superposition of the three maps shown in B shows that at this resolution ( $\sim 20$  Å) there is no significant difference in the observed epitope or binding angle of CH31 to the three different SOSIP trimers.



**B**

Ab	Ag	Temp (°C)	$k_a$ (1/Ms)	$k_d$ (1/s)	$K_D$ (M)	$K_D$ (nM)
CH31 Fab	CH505TF	11	2.92E+03	9.98E-05	3.42E-08	34.2
CH31 Fab	CH505TF	15	3.56E+03	1.80E-04	5.05E-08	50.5
CH31 Fab	CH505TF	20	4.83E+03	4.11E-04	8.52E-08	85.2
CH31 Fab	CH505TF	25	6.68E+03	9.98E-04	1.49E-07	149.3
CH31 Fab	CH505TF	30	1.05E+04	2.59E-03	2.47E-07	246.9
CH31 Fab	CH505TF	35	1.31E+04	8.12E-03	6.18E-07	617.8
CH31 Fab	CH505TF	40	1.42E+04	1.68E-02	1.18E-06	1181.6



**D**

Parameter	Value	SE
$\Delta H^\circ$ [kJ/mol]	-90.3	2.1
$\Delta S^\circ$ [J/(K*mol)]	-170.0	10.0
$T\Delta S^\circ$ [kJ/mol]	-50.7	3.0
$-T\Delta S^\circ$ [kJ/mol]	50.7	3.0
$\Delta G^\circ$ [kJ/mol]	-39.6	1.1
$\Delta C_p^\circ$ [kJ/(K*mol)]	-2.5	0.3

**Figure S4. Thermodynamic measurement of CH31 Fab binding to the CH505TF trimer by surface plasmon resonance (SPR), Related to Figure 1 and STAR Methods.** (A) Single-cycle kinetic titration sensorgrams of CH31 Fab binding to the CH505TF SOSIP trimer recorded at varying temperatures. Plots are representative examples of 3 replicate measurements. (B) Table of association rate constants ( $k_a$ ), dissociation rate constants ( $k_d$ ), and affinity constants ( $K_D$ ) recorded at varying temperatures. Values are reported as the average of 3 replicate measurements. (C) Plot of the natural logarithm of affinity ( $K_D$ ) versus the reciprocal temperature and non-linear van't Hoff fit. (D) Table of thermodynamic parameters obtained from non-linear van't Hoff analysis. Values are reported as the average and standard deviation of 3 replicate measurements.

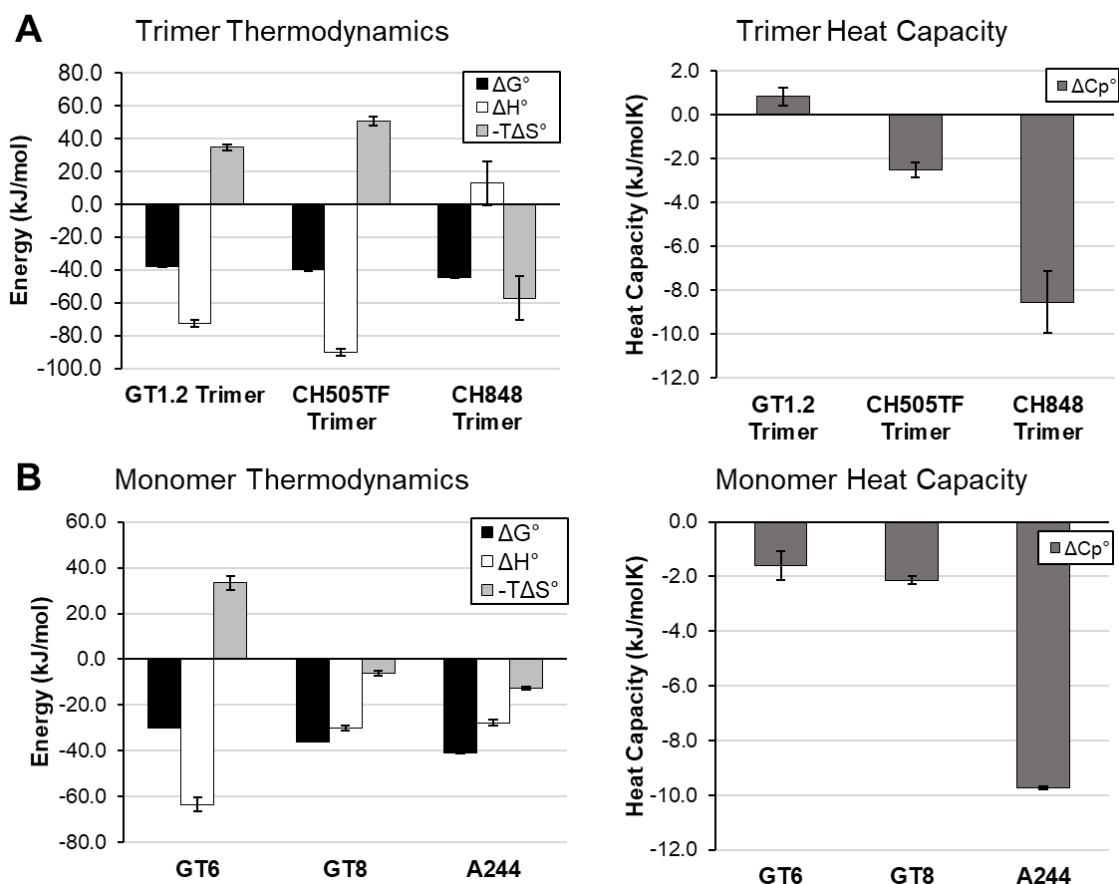


**Figure S5. Thermodynamics of CH31 binding to SOSIP trimers and monomeric antigens, Related to Figure 1 and STAR Methods.** (A) Thermodynamic analysis of CH31 Fab binding to GT1.2, CH505TF, and CH848 trimers revealed markedly different binding profiles. The similar affinity GT1.2 and CH505TF trimers exhibited entropy-enthalpy compensation where the interaction was driven by strongly favorable binding enthalpies ( $\Delta H < 0$ ) and offset by unfavorable binding entropies ( $-T\Delta S > 0$ ). The faster on-rate ( $k_a = 2.2 \times 10^5 \text{ M}^{-1}\text{s}^{-1}$ ) GT1.2 trimer displayed a relatively lower entropic hurdle ( $-T\Delta S$ ) and a negligible  $\Delta C_p$ , which suggests that minimal conformational changes occur during the association process. Therefore, the GT1.2 trimer and CH31 Fab exist in unliganded states that require no conformational rearrangement to form a productive encounter complex. Alternatively, the high affinity CH848 trimer exhibited a strongly favorable binding entropy ( $-T\Delta S < 0$ ) that is offset by a positive binding enthalpy ( $\Delta H > 0$ ) and a large, negative  $\Delta C_p$ . These data suggest that extensive conformational changes occur during association resulting in the slow association and dissociation rates observed for the highest affinity trimer. (B) A similar thermodynamic analysis of CH31 binding to the GT6, GT8, and A244 monomeric antigens also suggests varying binding mechanisms. The moderately fast association rate, weak affinity GT6 ( $k_a = 4.0 \times 10^4 \text{ M}^{-1}\text{s}^{-1}$ ,  $k_d = 2.1 \times 10^{-1} \text{ s}^{-1}$ ,  $K_d = 5247 \text{ nM}$ ) demonstrates a strongly favorable binding enthalpy ( $\Delta H \ll 0$ ) that is offset by an unfavorable binding entropy ( $-T\Delta S > 0$ ), whereas the fast association rate, moderate affinity GT8 ( $k_a = 2.3 \times 10^5 \text{ M}^{-1}\text{s}^{-1}$ ,  $k_d = 7.0 \times 10^{-2} \text{ s}^{-1}$ ,  $K_d = 307.8 \text{ nM}$ ) demonstrates a favorable binding enthalpy ( $\Delta H < 0$ ) and a favorable binding entropy ( $-T\Delta S < 0$ ). Both antigens bind with small  $\Delta C_p$  values indicating that minimal conformational changes occur during binding. In contrast, despite a similar thermodynamic profile to GT8, the slow on-rate, high affinity A244 antigen ( $k_a = 2.4 \times 10^3 \text{ M}^{-1}\text{s}^{-1}$ ,  $k_d = 7.3 \times 10^{-5} \text{ s}^{-1}$ ,  $K_d = 30.5 \text{ nM}$ ) exhibits a strongly negative  $\Delta C_p$  indicating

extensive conformational change is required to facilitate the bound complex. The observed relationship between thermodynamic conformational hurdles and antigen association kinetics provides further support to a kinetic model for B cell activation. Values and error bars represent the average and standard deviation of three measurements.

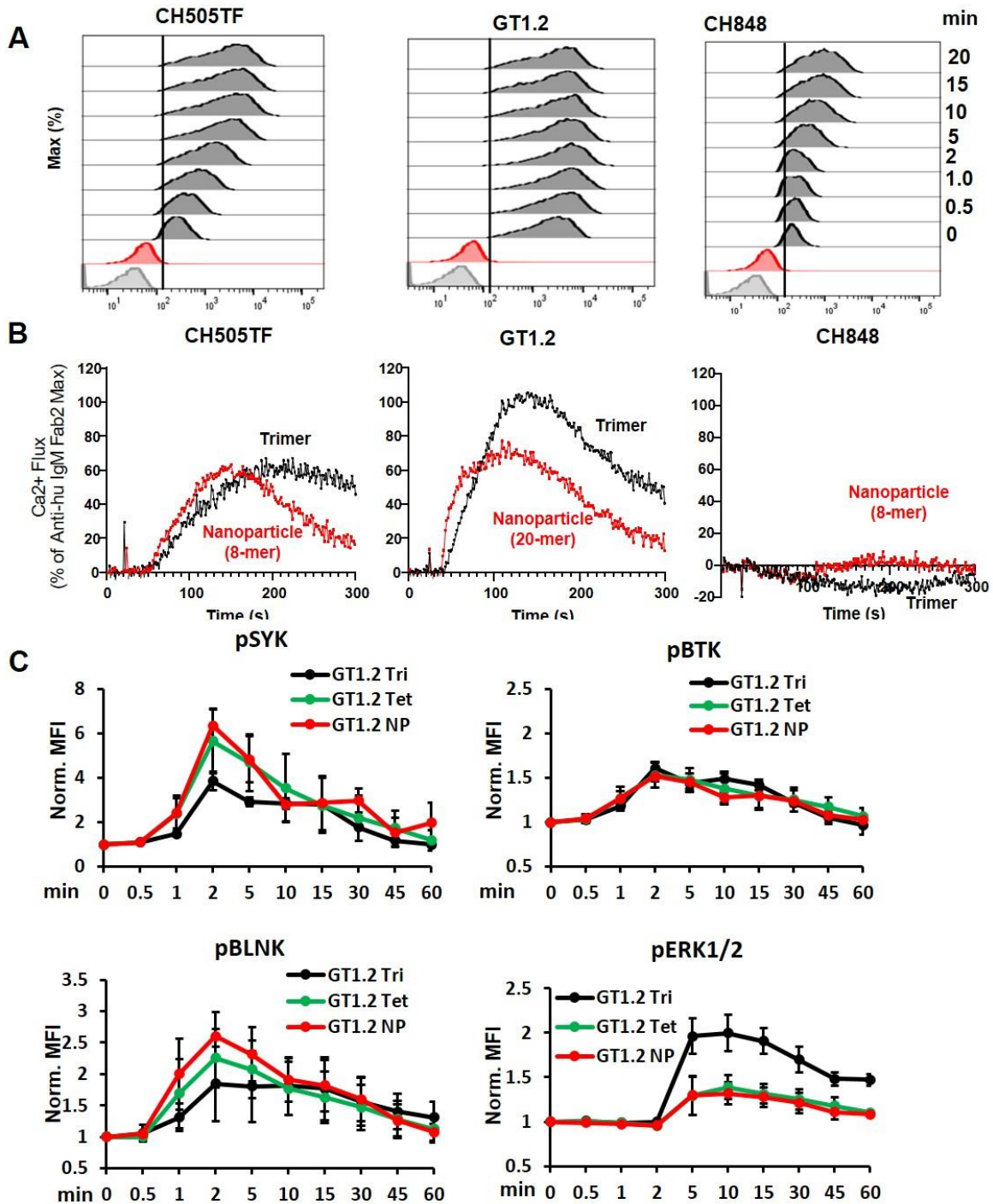


**Figure S6: Cell surface binding and signaling induced by SOSIP trimers and multimers of trimers, Related to Figure 2 and STAR Methods.** (A) Representative flow plots showing binding of CH505TF, GT1.2 and CH848 trimers to CH31 IgM BCRs over a period of 20 mins. Cells were stimulated with the biotinylated trimeric antigens at 30 nM concentration at 37°C and aliquots of cells were collected at the



indicated timepoints which further fixed and stained by anti-biotin antibody to analyzed in flow cytometer. **(B)** Comparison of the CH31 IgM Ramos cell activation induced by three trimeric antigens versus their nanoparticle forms. Results include (from left to right) CH505TF trimer (black) compared with the CH505TF ferritin nanoparticle (8-mer) (red); the calcium flux induced by the GT1.2 Trimer (black) compared with the GT1.2 nanoparticle (20-mer) (red); and the signaling mediated by the CH848 trimer (black) compared with its ferritin nanoparticle (8-mer) (red). Trimer and nanoparticle antigens for B cell activation were used at the same per unit trimer concentrations. Results are presented as a % of the maximum Anti-human IgM F(ab')<sub>2</sub> response and are representative of at least two measurements. **(C)** B cell signaling kinetics by multimers of GT1.2 trimer antigen stimulation. The kinetics of proximal Syk, BLNK, Btk and ERK1/2 phosphorylation in CH31 IgM Ramos cells were measured over an hour of stimulation by GT1.2 trimer (black), tetramer of GT1.2 trimer (green) and 20-mer of GT1.2 trimer (red) at 30 nM concentration. Around 2.5x 10<sup>5</sup> cells were collected at each indicated period of times, fixed (30 mins), permeabilized and then stained for phosphorylated Syk, BLNK, Btk and ERK1/2 and analyzed by BD LSRII flow cytometer. Plots shown here is normalized MFI data from three independent experiments. At each time point, the phosphorylation was normalized to the unstimulated cells MFI value (normalized value =1 for the unstimulated, unphosphorylated subset). Error bar indicate standard deviation of means.

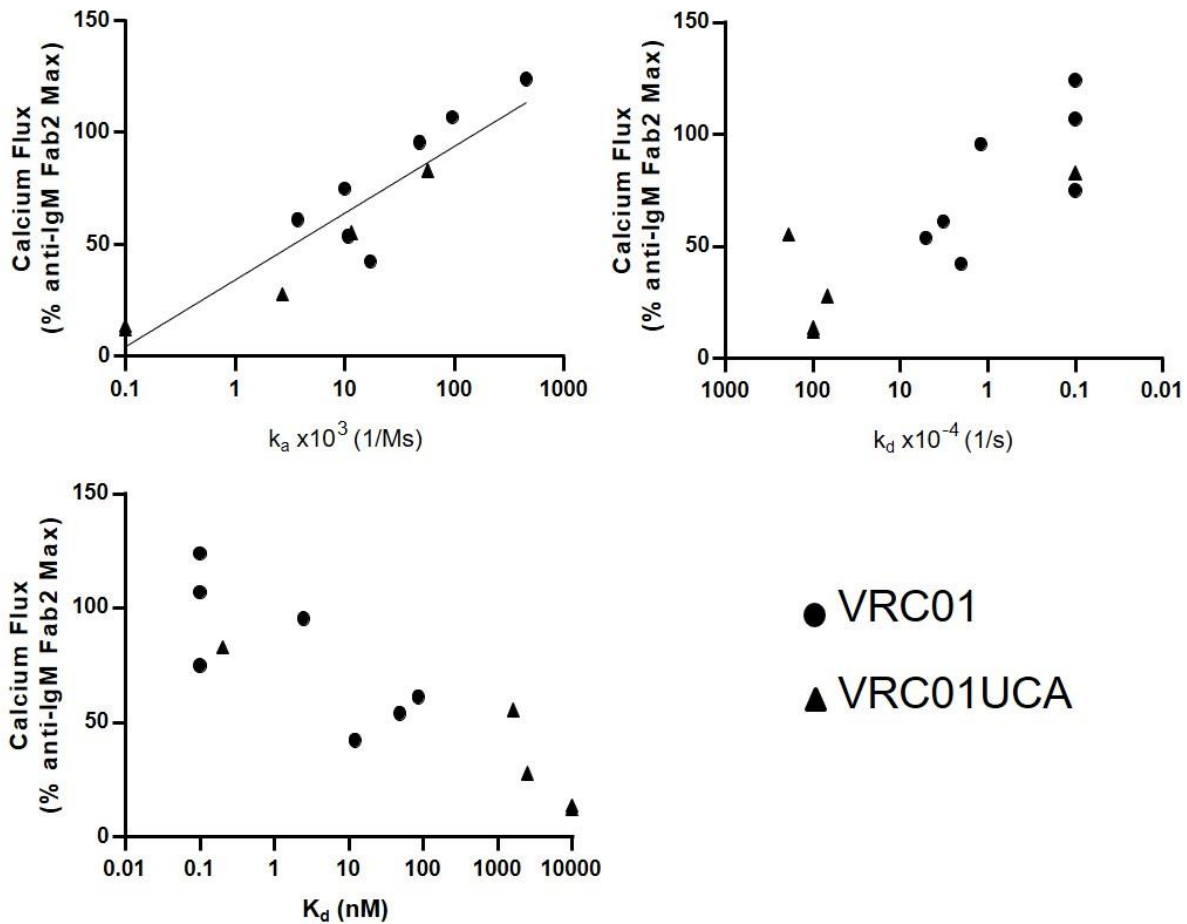


**Figure S7. Relationship between calcium flux response and antigen binding kinetic rates for VRC01 and VRC01UCA Ramos cell lines, Related to Figure 3 and STAR Methods.** VRC01 and VRC01UCA IgM Ramos cell calcium flux mediated by multimerized antigens (y-axis) plotted versus SPR measured monomeric (or trimeric) antigen on-rate ( $k_a$ , 1/Ms) (top left), off-rate ( $k_d$ , 1/s) (top right) or affinity ( $K_d$ , nM) (bottom left) against VRC01 or VRC01UCA bnAb (x-axis). Calcium flux responses are presented as a percentage of the maximum Anti-human IgM F(ab')<sub>2</sub> mediated responses and both calcium flux and kinetic rate parameters are representative one measurement for VRC01/VRC01UCA results. Correlation evaluation was assessed by Kendall's Tau analysis ( $k_a$  and VRC01 UCA: Kendall's Tau 0.9487; p-value = 0.0230;  $k_d$  and VRC01 UCA: Kendall's Tau -0.9487; p-value = 0.0230). The association between  $K_d$  and VRC01UCA IgM Ca-flux did not reach significance ( $K_d$  and VRC01: Kendall's Tau -0.6172; p-value = 0.0599).

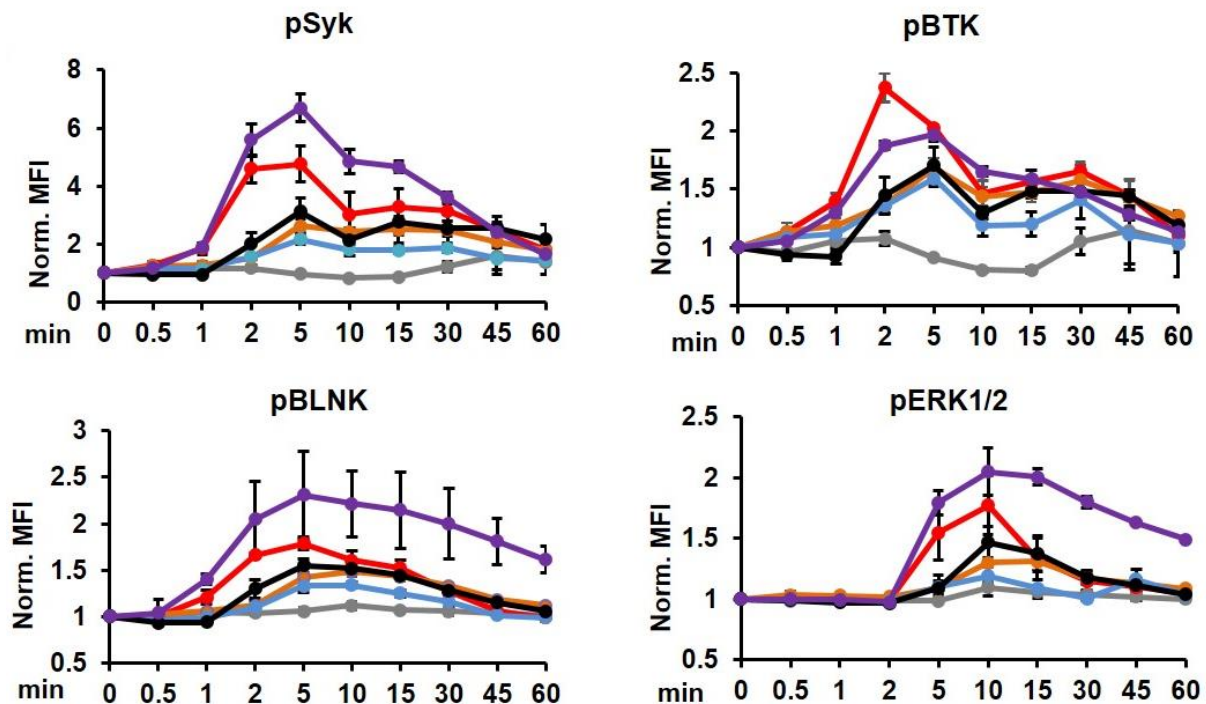


**Figure S8. CH31 IgM B phospho signaling by tetrameric antigens, Related to Figure 4 and STAR Methods.** B cell signaling kinetics by tetramers of gp120 based antigen stimulation. The kinetics of proximal Syk, BLNK, Btk and ERK1/2 phosphorylation in CH31 IgM Ramos cells were measured over an hour of stimulation by GT6 (grey), GT8 (red), A244 (orange), CH505TF (blue) and 426c (black) at 250 nM concentration along with anti-human IgM (purple) at 30 nM concentration. Around  $2.5 \times 10^5$  cells were collected at each indicated period of times, fixed (30 mins), permeabilized and then stained for phosphorylated Syk, BLNK, Btk and ERK1/2. Plots shown here is normalized MFI data from three independent experiments. At each time point, the phosphorylation level was normalized to the unstimulated cells MFI value (normalized value =1 for the unstimulated, unphosphorylated subset). Error bars indicate standard deviation of means.

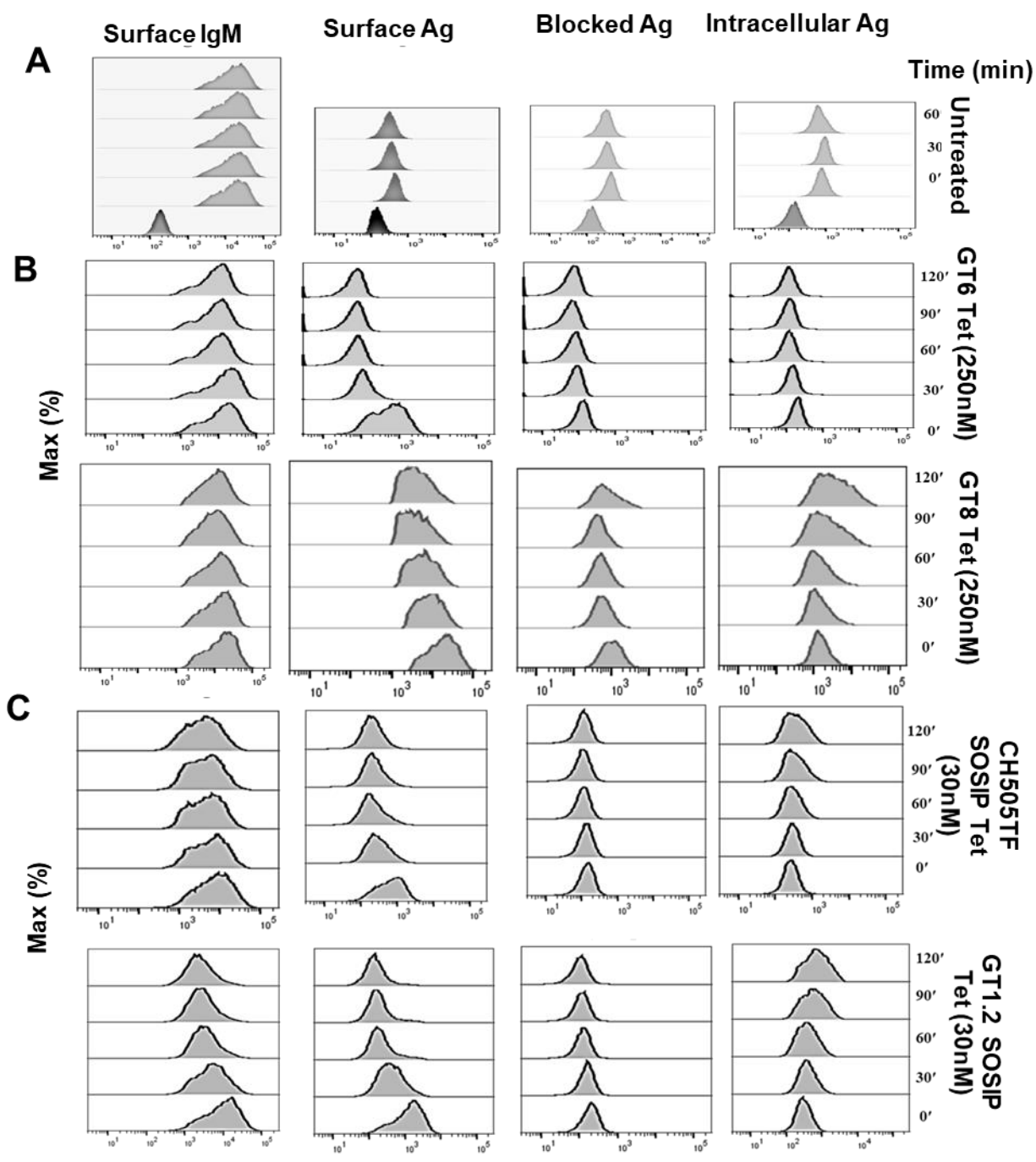


**Figure S9. Flow cytometric detection of intracellular antigens in CH31 IgM Ramos cells, Related to Figure 7 and STAR Methods.** Representative flow plots showing level of surface IgM, surface antigens, blocked antigens and intracellular antigens detected over time in ramos cells incubated with SA-conjugated tetramers of gp120 based antigens (B) and tetramer of trimeric antigens (C) or left untreated (A). Level of surface IgM and bound antigens were detected at each time points using fluorophore conjugated anti-IgM and anti-SA antibody respectively. To block the SA-binding sites on surface antigens, cells were incubated with non-fluorophore anti-SA antibody and blocked level of SA binding sites were confirmed. For intracellular antigen detection, cells were fixed and permeabilized after surface blockage of SA binding sites and further incubated with fluorophore conjugated anti-SA antibody and analyzed by flow cytometry.

CH31 IgG mAb				
Ag	Assay Temp (°C)	Monomer/Trimer (RU)	Tetramer (RU)	Response (RU) Fold Change
426c degly3	25	7.8	105.9	13.6
GT6	25	24.2	95.6	4.0
GT8	25	69.5	137.8	2.0
CH505TF	25	65.2	98.6	1.5
426c	25	62.5	278.7	4.5
A244	25	57.7	51.0	0.9
CH505TF Trimer	37	243.6	276.0	1.1
GT1.2 Trimer	37	570.4	593.5	1.0

**Figure S10. Response fold change of antigen monomers/trimers versus multimers, Related to Figure 5 and STAR Methods.** Summary table comparing the SPR binding responses (RU) to CH31 IgG bnAb of monomeric antigens (or trimeric) with the binding responses of their multimeric (4-mer) forms. The responses were measured at the end of the association phase of the sample injection and the fold change between the antigen types was calculated by dividing the response of the tetramer by the response of the monomer (or trimer). The 426c degly3 and 426c core proteins exhibited the largest increase in binding response against CH31 IgG after tetramerization. GT6, GT8, and CH505TF gp120 all showed some enhancement in binding (1.5x or greater) after tetramerization while A244, CH505TF trimer, and GT1.2 trimer showed little to no increase in binding.

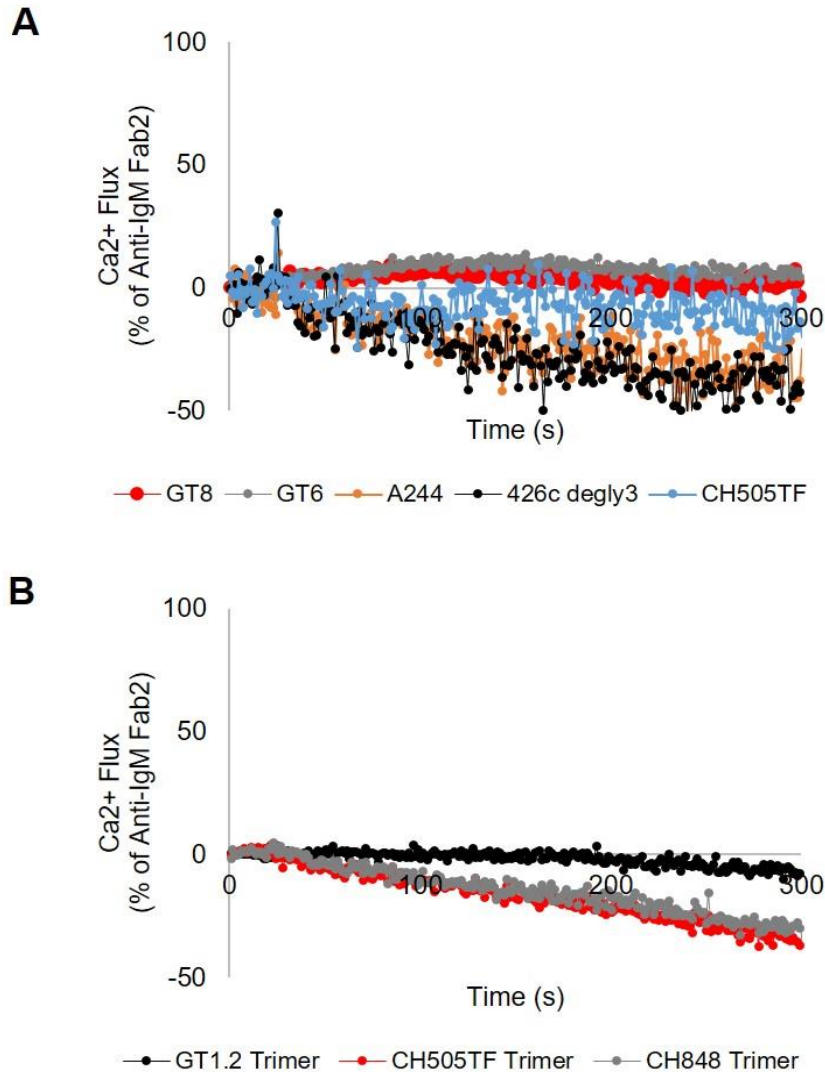


**Figure S11: Negative control CH65 IgM B cell signaling by tetrameric and trimeric Env proteins, Related to STAR Methods.** (A) Overlaid calcium flux responses of the negative control Ramos cell line expressing the flu HA-specific IgM BCRs (CH65) induced by the following tetrameric versions of monomeric proteins: GT6 (grey), GT8 (red), A244 (orange), CH505TF (blue) and 426c (black). The tetramers were prepared at the same per unit monomer concentration (1 $\mu$ M). Results are presented as a % of the maximum Anti-human IgM F(ab')<sub>2</sub> response and are representative of at least one measurement. (B) Comparison of CH65 IgM Ramos cell activation induced by three trimeric antigens: CH505TF trimer (red), GT1.2 Trimer (black), and CH848 trimer (gray). Trimers were prepared at 1 $\mu$ M (per unit trimer). Results are presented as a % of the maximum Anti-human IgM F(ab')<sub>2</sub> response and are representative of at least two measurements.

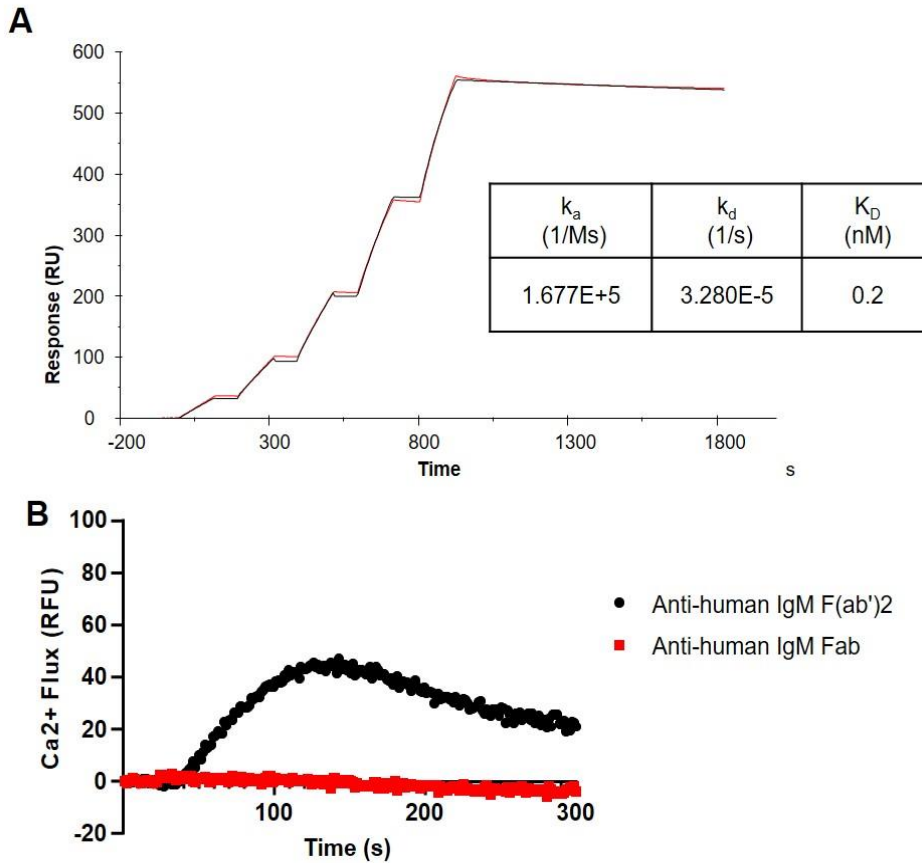
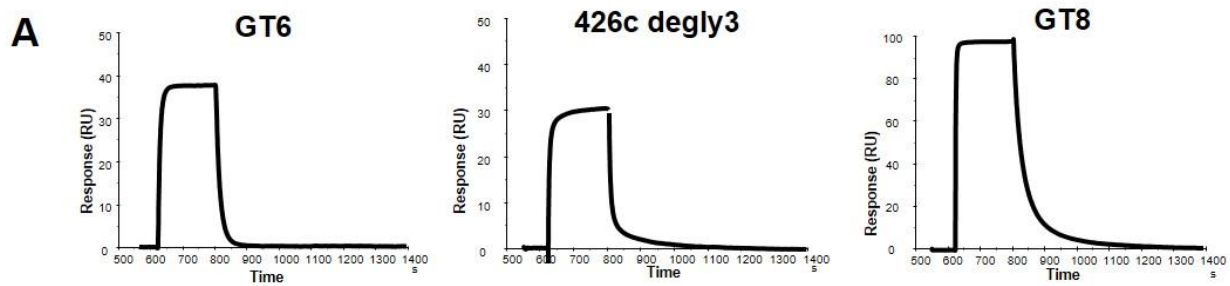


**Figure S12. CH31 IgM mAb and IgM Ramos cell line analysis with control stimulants, Related to Figure 1 and STAR Methods.** (A) SPR single cycle kinetic binding profile of the positive control anti-human IgM F(ab')<sub>2</sub> against CH31 IgM. The results are representative of two measurements. (B) Calcium flux of CH31 IgM Ramos cells by the dimeric stimulant Anti-human IgM F(ab')<sub>2</sub> (black) and the monomeric Anti-human IgM Fab (red) at 50ug/mL. The fluorescence of a blank well containing only RPMI/dye was used for background subtraction. The calcium flux profiles are representative of at least two measurements.



**B**

Ag	Assay Temp (°C)	Monomer $k_d$ (1/s)	Monomer $t_{1/2}$ (min)
GT6	25	2.5E-1	0.05
	15	1.2E-1	0.09
426c degly3	25	6.1E-1	0.02
	15	6.9E-2	0.2
GT8	25	6.8E-2	0.2
	15	2.2E-2	0.5

**Figure S13. Effect of temperature on binding dissociation rates, Related to Figure 5 and STAR**

**Methods.** (A) SPR binding curves of monomeric proteins to CH31 IgG measured at 15°C. The plots are representative of three measurements. (B) Env protein binding off-rates ( $k_d$ , 1/s) and half-life ( $t_{1/2}$ ) of antibody-bound complex to CH31 IgG. Protein-antibody half-life ( $t_{1/2}$ ) were derived from  $k_d$  values using  $t_{1/2} = \ln(2)/k_d$ . Binding curves as well as  $k_d$  and half-life measurements are representative of at least two measurements.